Lyman Alpha Forest

See annual review article (ARA&A) by Rauch (1998) for more discussion and text. A useful (but basic) introductory website is http://astron.berkeley.edu/~jcohn/lya.html

1 History

The Lyα forest is the region of numerous, weak lines seen bluewards of the QSO's Lyα emission. Below $(z+1)*1025$ Å there are also Lyβ lines and so on down the Lyman series. Higher order lines are weaker (lower f values) than Lyα but at blue wavelengths the combination of Lyα and high order lines leads to a very high line density. A few of the lines in the forest are due to metals (see later). We already discussed the various pieces of evidence that led us to understand that the Lyα forest is mostly made up of *intervening* systems.

Early theoretical models considered individual 'clouds' that were confined either by gravity or pressure from the ICM. Now our picture is of a fluctuating medium.

1.1 Pressure Confinement

This model is based on a 2 phase medium – a hot intra-cloud medium (ICM) in pressure equilibrium with cooler denser Lyα clouds. Lyα clouds are in photoionization equilibrium with an ionizing background, a sort of inverted Stromgren sphere. Gas is heated by the background and cools via thermal bremsstrahlung (free-free absorption of a photon by an electron), compton cooling (high energy electron transfers energy to photon in collision), the usual recombination and collisional excitation processes and constant adiabatic cooling due to the expansion of the universe. The ICM is constantly cooling due to adiabatic expansion, because the high degree of ionization does not allow for efficient photoionization heating (i.e. bound-free heating). However, the denser clouds expand isothermally with $T \sim 3 \times 10^4$ K until the density drops sufficiently that photo-heating can no longer compensate for work of expansion. The clouds now start to cool and the sound speed ($v = \sqrt{\gamma RT/M}$ where gamma is the adiabatic constant) in the gas therefore drops so that pressure equilibrium with the ICM is lost and the clouds enter free expansion and are ultimately destroyed. Dense clouds in a hot ICM formed at $z \sim 6$ could survive until $z \sim 4$ if they had $10^5 < M < 10^{10}$ $M_\odot$. Problems with pressure confinement scenario:

1. No evidence for absorption associated with the ICM
2. To reproduce the CDDF, need 'clouds' with masses spanning nine orders of magnitude whereas lifetimes restrict this to 4.

1.2 Gravitational Confinement

Two main models - self-gravity (baryonic) or CDM mini-halos. The former never really took off because it required extremely large clouds and couldn't reproduce observations e.g. the CDDF. Confinement in mini-halos seemed a natural product of the CDM model. Photoionized gas settled into a DM halo and is stably confined if the potential is shallow enough to avoid gravitational collapse, but deep enough to stop warm gas escaping.

One attraction of this model was that the CDDF was naturally reproduced by the strong dependence of density on impact parameter, rather than an intrinsic range of cloud properties. This led to the suggestion that the power law CDDF indicated that all QALs were the same beast.

1.3 Hydrodynamic Simulations

A more sophisticated view of this picture came with cosmological hydrodynamical simulations. One problem with the minihalo model model is that most virialized objects have radii ~ 10 kpc, much smaller than the sizes inferred from multiple lines of sight. Hydrodynamical simulations changed this picture by letting gas follow the distribution of DM without having settled into virialized structures.

Note that a 'line' of given N(HI) represents a very different structure at different redshifts, because the mean density of the universe decreases with time. Overdensity is defined as

$$\delta = \rho/\overline{\rho(z)} - 1 \tag{1}$$

A line with log N(HI) = 14 might represent the mean density at say $z \sim 5$, but at $z \sim 1$, this is a very overdense filament. We must therefore be careful with comparisons at different redshifts.

Is Voigt profile fitting realistic if clouds are not discrete? Non-voigtness is detected, but this still represents a convenient parameterization of the data. Siumlations also show us that optical depth is proportional to overdensity; at $z \sim 3$ an optical depth $\tau = 1$ probes gas of about the mean density.

2 Statistical Properties

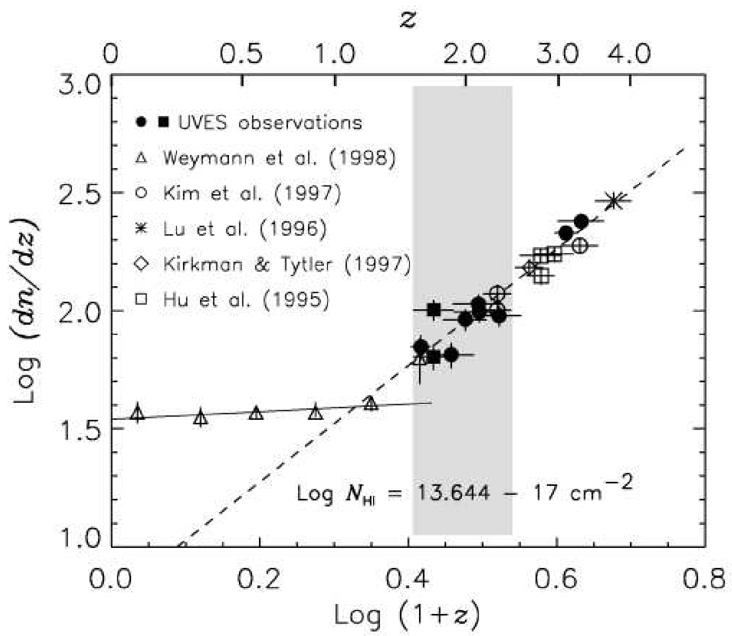

Figure 1: Evolution of Lyα forest number density taken from Kim et al 2002.

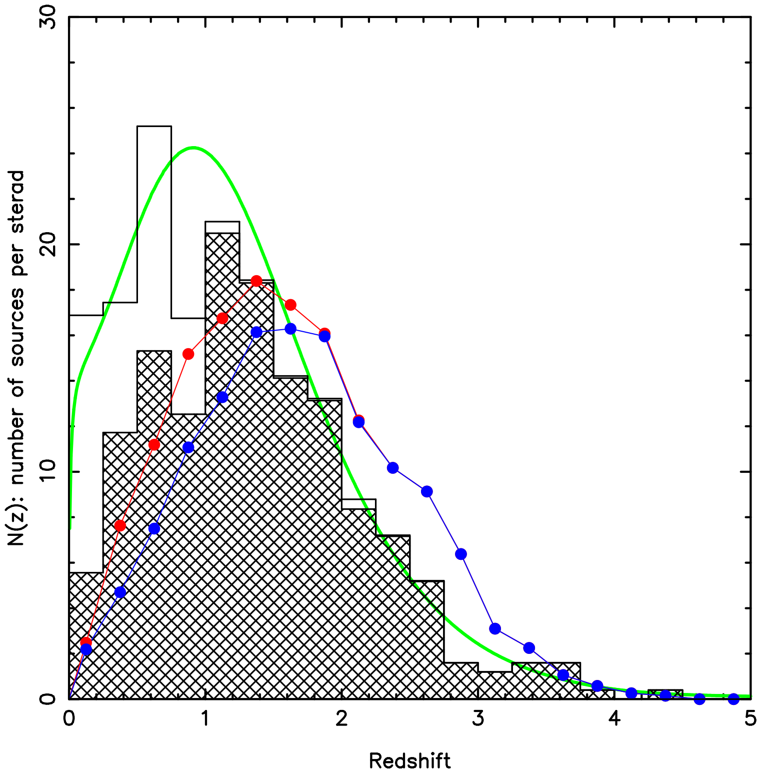

Figure 2: Evolution of the space density of QSOs (hatched histogram) - partly responsible for change in n(z) of Lyα absorbers, Wall et al. (2005).

We have already seen that the CDDF is a power law with slope around -1.5. As we saw in the last lecture, looking at the number density as a function of redshift can tell us whether the population is evolving. I.e. determine the index γ in

$$n(z) = n_0(1+z)^\gamma \tag{2}$$

N(z) evolves with redshift with a break at around $z \sim 1.7$. The evolution is governed by two physical processes - Hubble expansion and evolution of ionizing flux. Hubble expansion dominates at high z where the QSO flux is approximately constant, but QSO space density drops at $z \sim 2$. Now, the expansion is somewhat offset by a lower ionizing background, so more clouds can remain neutral. However, the break also occurs at the redshift where space observations are required, could this be an instrumental affect? No - Kim et al (2002) have pushed ground based observations with UVES down to HST regime, and the match is good. The evolution depends on the N(HI) regime - high N(HI) systems seem to evolve more rapidly. This could be due to blending of the low N(HI) lines, or incompleteness at high z. In any case, the forest is 'thicker' at high redshifts, hence line blanketing becomes serious in $z > 5$ QSOs.

γ appears to depend on column density, which is not predicted by simulations. This dependence could be due to incompleteness or blending at low N(HI) at high z, as well as real changes in the forest. The latter would imply that high N(HI) systems evolve more rapidly.

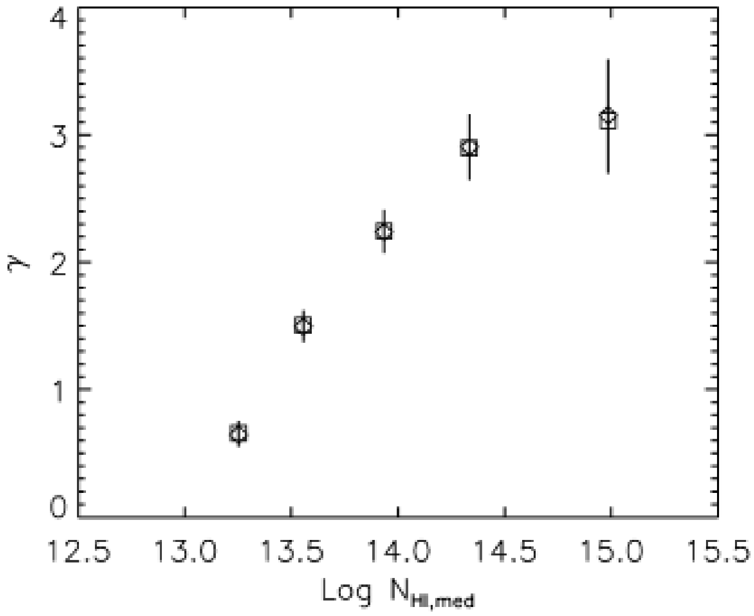

Figure 3: Evolution γ as a function of N(HI) taken from Kim et al 2002. This could be due to line blending/incompleteness and/or real differences in evolution.

3 Physical Properties

3.1 Clustering of the Lyα Forest

Insights into the spatial properties of the Lyα forest come from transverse sizes and and LOS two-point correlation function (TPCF).

$$\xi(\Delta v) = \frac{N_{obs}(\Delta v)}{N_{exp}(\Delta v)} - 1 \tag{3}$$

Note that to change a difference in redshifts into a velocity:

$$v = \frac{\Delta z}{z+1} \times c \tag{4}$$

And to calculate co-moving sizes from velocities (applicable over non cosmological distances)

$$\frac{v}{c} = \frac{d(Mpc)}{3000h^{-1}} \tag{5}$$

The TPCF compares the number of observed lines in a given velocity range with the number expected from a random distribution. Find sizes of a few Mpc, consistent with simulations. Can also find voids using this method, up to 20 Mpc in size. In general, Lyα is less clustered than galaxies, although clustering does increase with N(HI).

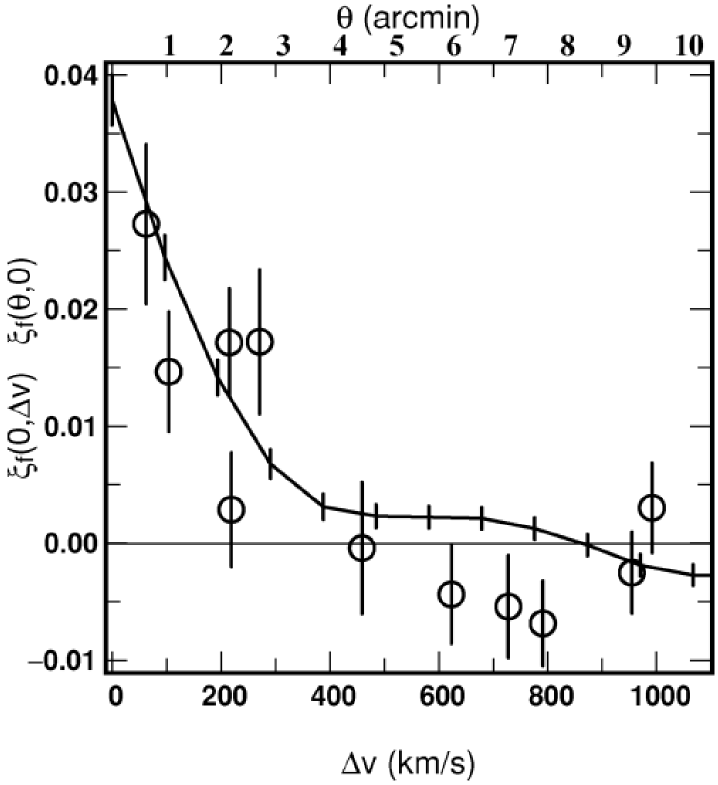

Figure 4: Two point correlation function of the Lyα forest from Rollinde et al (2003). Vertical ticks show transverse scale, circles are line of sight.

3.2 Temperature of the Lyα Forest

The temperature of the IGM can be inferred through the b-values of the Lyα and associated metal lines. Recall that b-values have contribution from the thermal and turbulent motions, these can be separated if two different elements (e.g. CIV and SiIV) are observed:

$$b_{x,y}^2 = b_{turb}^2 + \frac{2kT}{m_{x,y}} \tag{6}$$

for two elements, x and y. This can be easily solved to give

$$b_{therm}^2(CIV) = \frac{b^2(CIV) - b^2(SiIV)}{1 - m(C)/m(Si)} \tag{7}$$

Typical temperatures inferred from this method are $\sim$ 40,000 K. In the absence of metal lines, the situation is more complex and requires explicit modelling. However, the physics in the low density IGM is relatively straightforward and since there is no shock-heating the combination of adiabatic cooling and photo heating results in an equation of state (temperature density relation) which is a power law (note this is a bit of a mis-nomer because the equation of state usually only applies to an ideal gas). Since shocking heating is unimportant in a low density gas, there is a balance in adiabatic cooling and photo-heating such that the temperature depends on the overdensity:

$$T = T_0(\rho/\overline{\rho})^{\gamma-1} \quad (8)$$

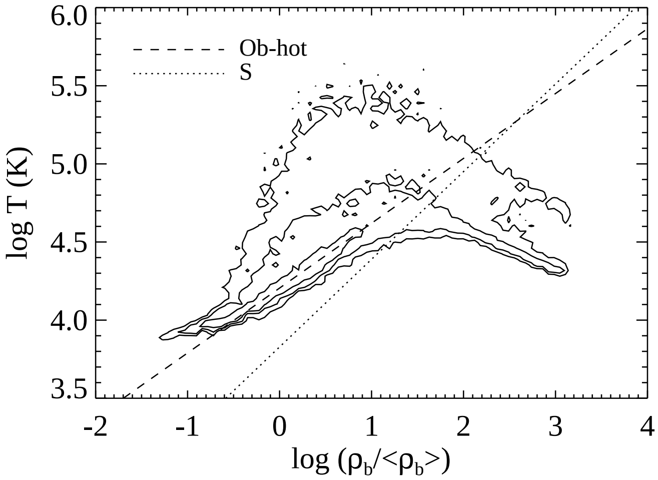

Figure 5: Correlation (based on simulations) of overdensity and T in the IGM (taken from Schaye et al. 1999). Contour levels are for actual densities. The fact that the low density gas follows a tight power law leads to a simple equation of state.

where T_0 is the temperature at the mean density. Even though the temperature can't be derived from a Lyα b-value directly (and there is the added complication that there is blending), the cut-off in their distribution is a good test of the temperature (since in the low column density Lyα forest the b-value is dominated by thermal, not turbulent, broadening and differential Hubble flow). So, the cut-off in b-value tells us about the equation of state and since the N(HI) tells us the optical depth and therefore the density, we can infer the temperature. Schaye et al (2000) found an increase in temperature at $z \sim 3$ which they attributed to ionization of He II $\rightarrow$ He III. If ionization happens abruptly, the gas is approximately isothermal and $\gamma \sim 1$. As time progresses the slope $(\gamma - 1)$ increases as the denser regions undergo less expansion and more photo-heating.

4 Proximity Effect

We have seen that, in general, the line density of the Lyα forest increases with redshift. However, in the early 1980s it was noticed that the line density actually dropped as it approached the redshift of the QSO. This is the proximity (or inverse) effect. It was quickly realised that this is due to the excess radiation field near the QSO which ionizes more of the IGM, so the mean absorption due to HI drops.

For a cloud with column density N(HI) exposed to only a background radiation field the observed N(HI)is

$$N'(HI) = \frac{N(HI)}{\int_{\nu_0}^{\infty} 4\pi J(\nu)} \quad (9)$$

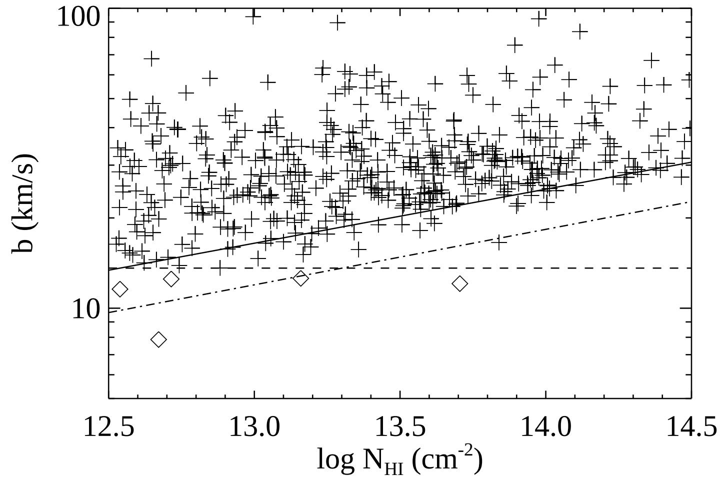

Figure 6: Cut-off in b-value distribution model with a power law fit to the equation of state.

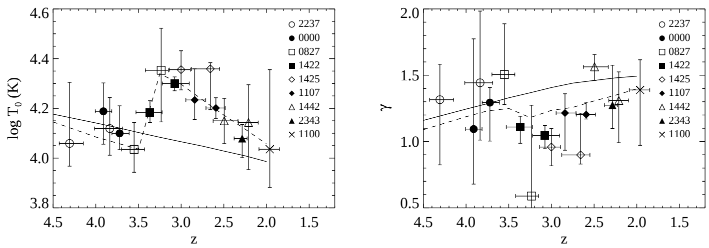

Figure 7: Evolution of temperature in the Lyα forest from Schaye et al. (2000).

where $J(\nu)$ is the mean intensity of the background in units of erg/s/cm^2/ster/Hz and should be summed over all frequencies from the Lyman limit. N(HI) is the column the cloud would appear to have in the absence of an ionizing background. If a bright QSO is present there is also a contribution from the local flux

$$N''(HI) = \frac{N(HI)}{\int_{\nu_0}^{\infty} 4\pi J(\nu) + F(\nu)} \tag{10}$$

where

$$F(\nu) = \frac{L(\nu)}{4\pi r^2} \tag{11}$$

We write the ratio of the QSO and background contributions as measured at 912 Å as

$$\omega = \frac{F(\nu_0)}{4\pi J(\nu_0)} \tag{12}$$

So the observed N(HI) with both background and QSO ionizing radiation is

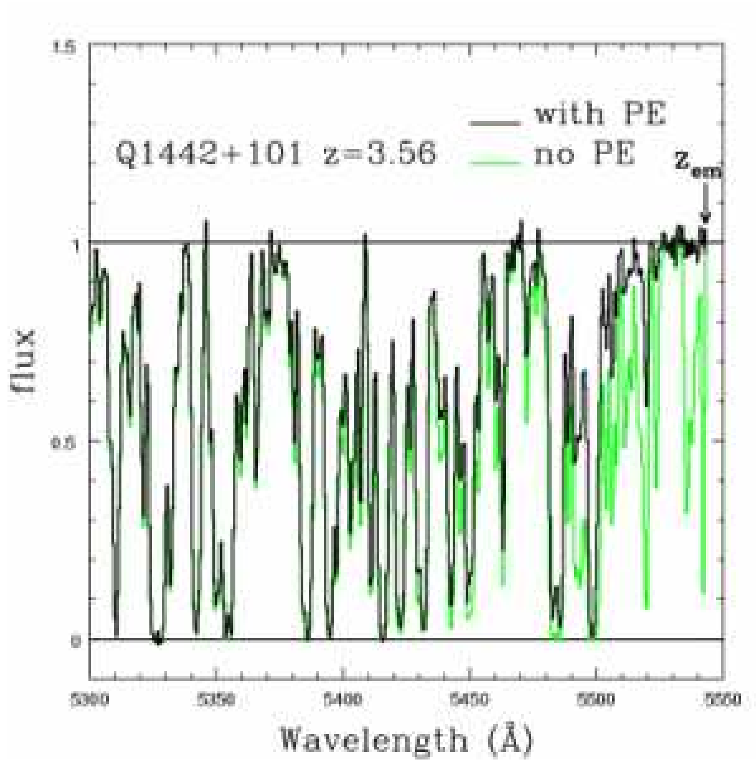

Figure 8: The proximity effect - few lines near the QSO due to photo-ionization.

$$N''(HI) = \frac{N'(HI)}{(1+\omega)} \tag{13}$$

i.e. observed N(HI) drops by a factor $(1+\omega)$. Think of ω as a distance from the QSO scaled by the ratio of contributions from the QSO and background ionizing fluxes, i.e. ω increases as we approach the QSO. The observed number of lines depends on both the number density and CDDF, so the number above a certain N(HI) threshold is given by:

$$dN/dz \equiv n(z) = A_0(1+z)^{\gamma}[1+\omega(z)]^{1-\beta} \tag{14}$$

where β is the slope of the CDDF. Use line counts as a function of r to determine ω and then $J(\nu)$ for a given EW limit. At small ω, as we get further from the QSO, n(z) reaches an asymptote as the radiation from the QSO becomes negligible. Often, we change from z to X to follow the evolution in co-moving coordinates

$$X_{\gamma} = \int (1+z)^{\gamma} dz \tag{15}$$

So in the absence of a proximity effect

$$n(z) = \frac{dN}{dX_{\gamma}} = A_0 \tag{16}$$

There has been a lot of disagreement in the value of $J(\nu)$. Some problems include

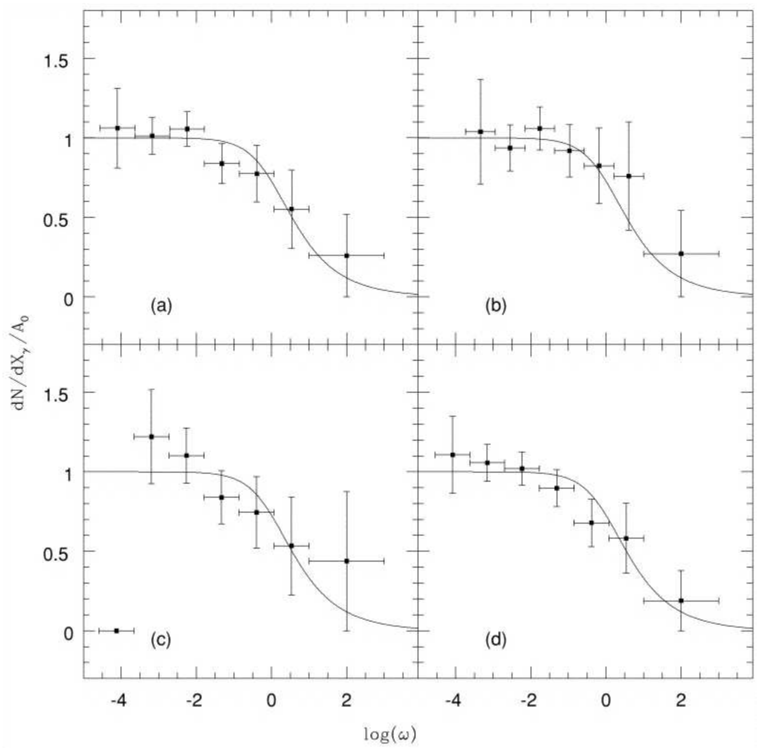

Figure 9: Proximity effect means that ω increases closer to the QSO and reaches an asymptotic value further away (Scott et al. 2002)

1. Knowing the true redshift of the QSO
2. Lines can be saturated
3. Lines can be blended
4. Relies on an assumed β

Can affect $J(\nu)$ by up to a factor of 2! In the range $2 < z < 4$ the amount of background ionizing radiation is about 2–3 times what we expect from QSOs. The extra flux may come from star forming galaxies which could produce one order of magnitude more Lyman continuum photons than QSOs. But what fraction escapes? If it were around 10% then the QSOs and galaxies would contribute approximately equally to photo-ionizing background; some observations (e.g. Steidel et al. 2001) have suggested there could be as much as five times more coming from galaxies.

Transverse proximity effect can also be studied.

The proximity effect is the reason that observing Lyα emitters at high z is not necessarily evidence that the universe was ionized at that epoch.

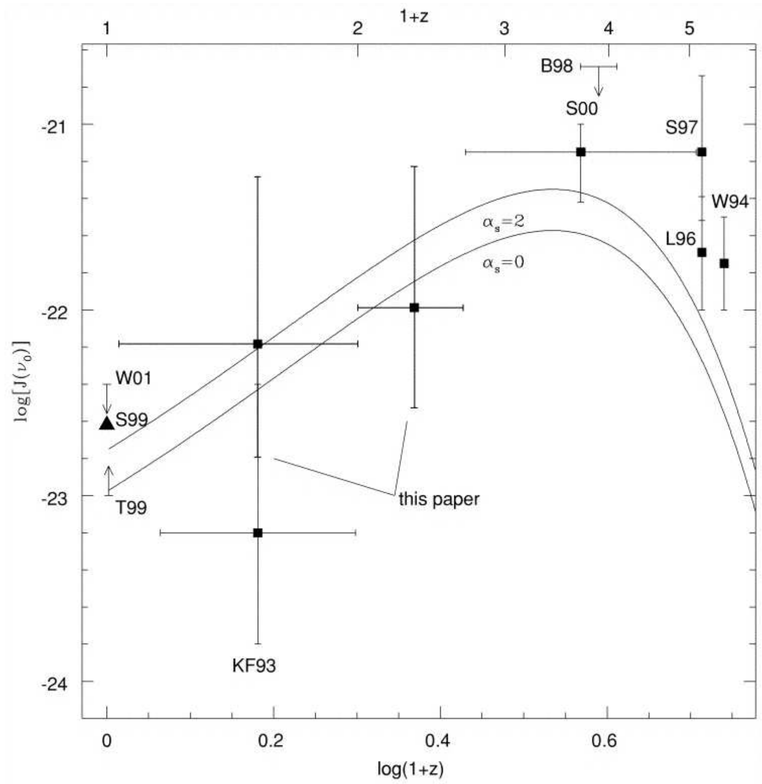

Figure 10: Proximity effect gives us photo-ionizing background as a function of redshift - Scott et al. (2002)

5 The Lyα Forest Galaxy Connection

5.1 Low Redshift Galaxy Associations

At low redshifts, the higher N(HI) Lyα clouds may be associated with galaxy halos. After all, the original interpretation of a single CDDF was a single population. However, there has been considerable debate about the association of galaxy halos with Lyα absorption. Can we relate individual Lyα clouds with a given galaxy, or do they trace a larger scale structure? On the one hand, many studies find Lyα absorption out to impact parameters of 300 kpc in the fields of galaxies at low and intermediate redshift. Some (e.g. Chen et al 2001) claim an anti-correlation between impact parameter (scaled for luminosity) and N(HI) (or EW). This is not reproduced by others (e.g. Bowen et al 2002) who point out the difficulty of associating a given galaxy to a particular absorber. Instead, Bowen et al. propose a correlation between total Lyα EW and number of galaxies in a given volume.

5.2 High Redshift Galaxy Associations

At high redshift, investigations between the Lyα forest and galaxies has been done using LBG searches in the fields of QSOs. The gas is traced along the single QSO line of sight per field and then galaxies matched to absorbers (allowing a certain velocity tolerance). Comparison with the neutral (Lyα) gas shows that there is generally more absorption near (within a few Mpc) of

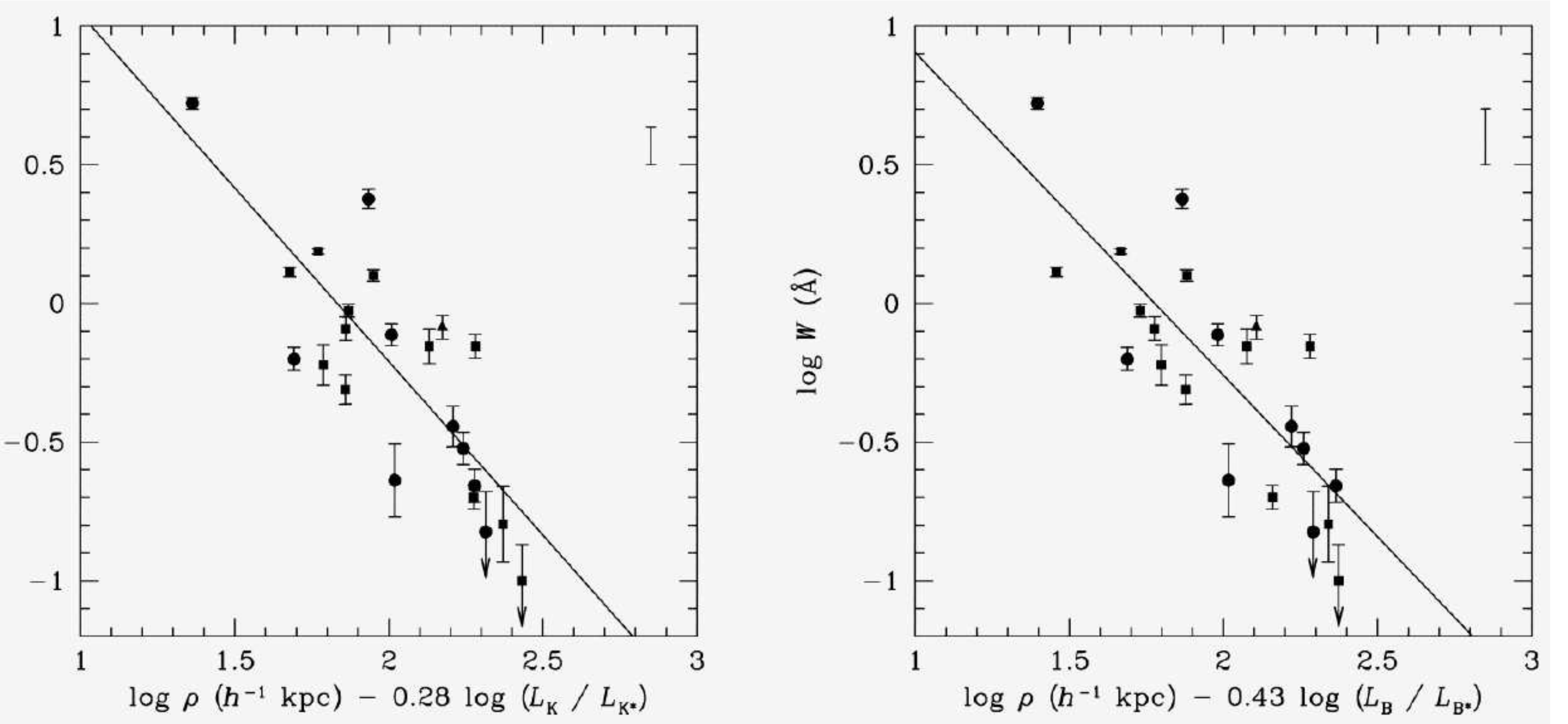

Figure 11: Chen et al. (2001) claimed that Lyα EW correlated with impact parameter scaled for luminosity.

galaxies, a correlation which peters out around 6 Mpc (co-moving). However, at small distances (a few hundred kpc) there is a dearth of absorption. This could be due to small number statistics or the velocity tolerance that is adopted (see Adelberger et al. 2003 for a full discussion). Alternatively, is it a proximity effect? Unlikely the stellar ionizing radiation could be so strong. Instead, a model of very strong (600 km/s or more) superwinds is suggested.

There is also evidence that CIV with N(CIV) $>$ 13.5 correlates with galaxies out to several hundred kpc. Does this have a large impact on transporting metals into the IGM?

6 Metals in the IGM

If the Lyα forest (at least at high z) is the IGM, we might expect it to contain 'pristine' material. The advent of high resolution spectrographs on 4-m telescopes showed this not to be the case. The CDDF of CIV is a power law which extends down to low N(CIV) with no sign of a turnover.

Can calculate the mass density of metals as a function of redshift out to $z \sim 5$.

$$\Omega(CIV) = \frac{Hm_{CIV}}{c\rho_{crit}} \int Nf(N)dN \tag{17}$$

There is little evolution - why? Could be that Most star formation at high z is in massive objects which retain more of their metals. Also have to remember that the 'objects' probed at different redshifts for a given N(HI) have different overdensities. Nevertheless, at some point at high z, should see a turnover.

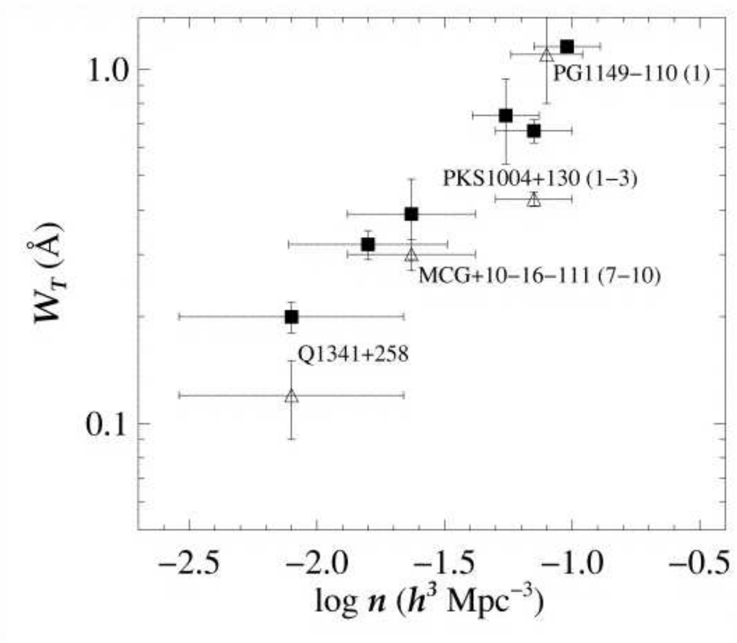

Figure 12: Local density of galaxies versus HI EW from Bowen et al. (2002).

Are these metals in galaxies or the IGM? Answer this by going to very low N(HI) (log N(HI) $\sim$ 13.5 corresponds to the mean density at $z \sim 3$). First approach tried stacking data - non-detection. However, this result is affected by small offsets in the redshifts of CIV and HI. Alternative approach is to use pixels, which is less affected by this shift and produces 1000s of data points for a single spectrum. This technique has revealed CIV and OVI in gas down to about the mean density.

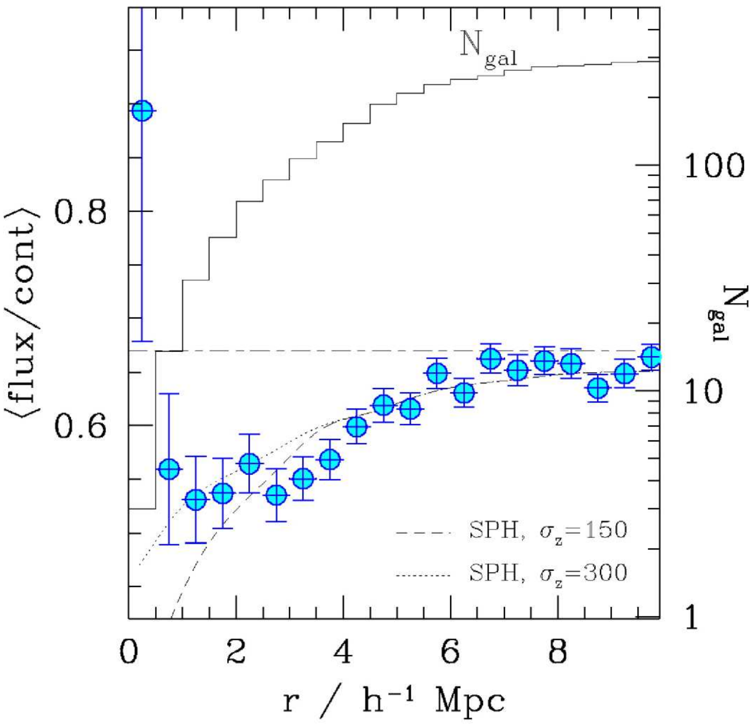

Figure 13: Excess of HI absorption (i.e. flux depression) near LBGs, except at the smallest separations. Taken from Adelberger et al. (2003).

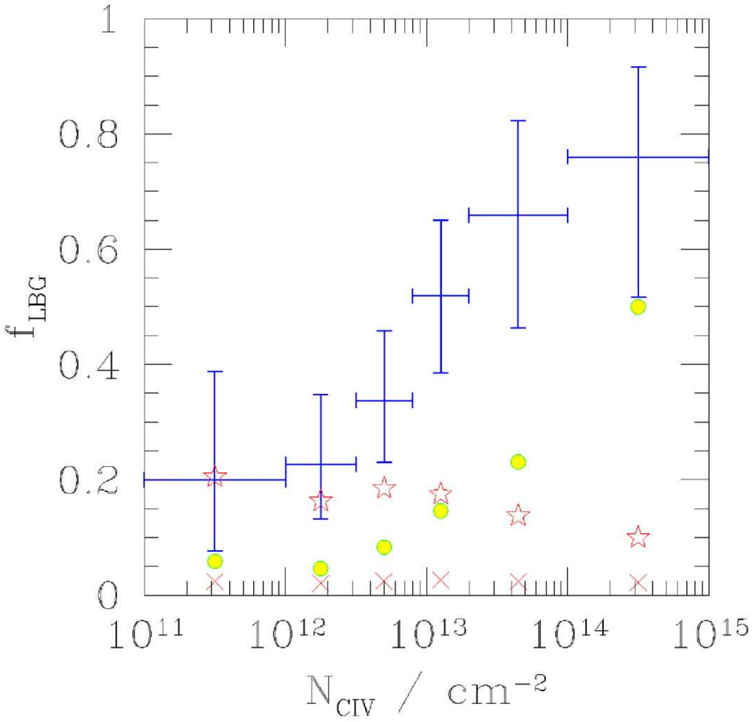

Figure 14: Fraction of CIV systems of a given N(CIV) that lie within 250 kpc of LBG. Small red crosses show expectation for random associations. Taken from Adelberger et al. (2003).

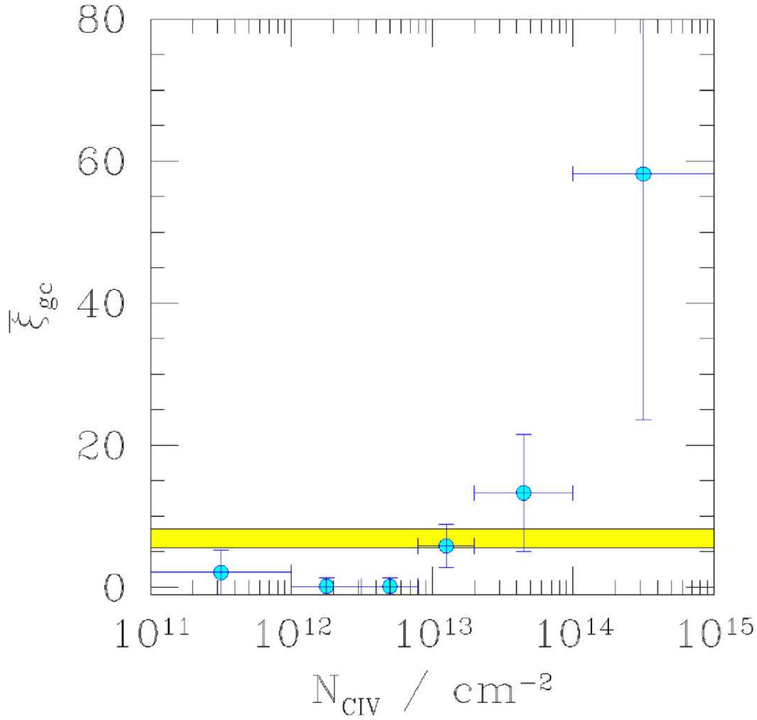

Figure 15: Overdensity of CIV systems associated with LBGs as a function of N(CIV). Horizontal band shows random distribution. Taken from Adelberger et al. (2003).

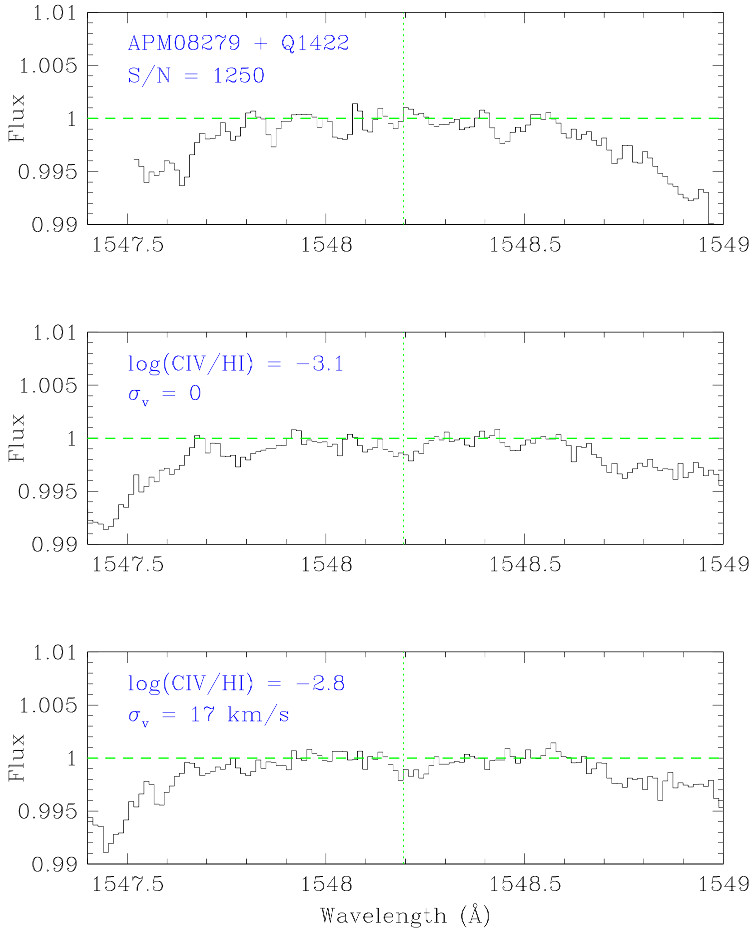

Figure 16: Stacking data to look for weak CIV depends critcally on whether there are small redshift shifts between Lyα and CIV (Ellison et al. 2000).

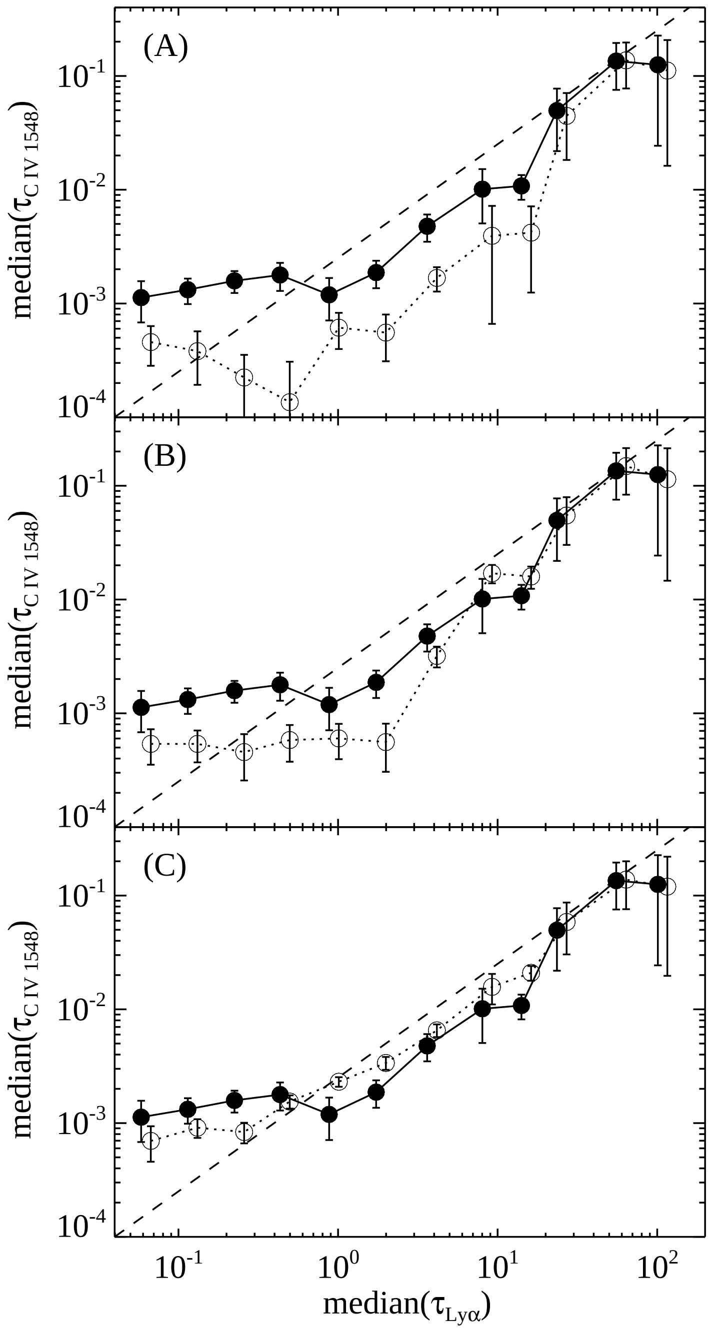

Figure 17: Looking for weak CIV with pixel optical depths (Ellison et al 2000). Panel A only has strong CIV systems, panel B has CIV below detection limit but asociated with only high N(HI) absorbers, panel C has CIV in even the weak Lyα clouds.

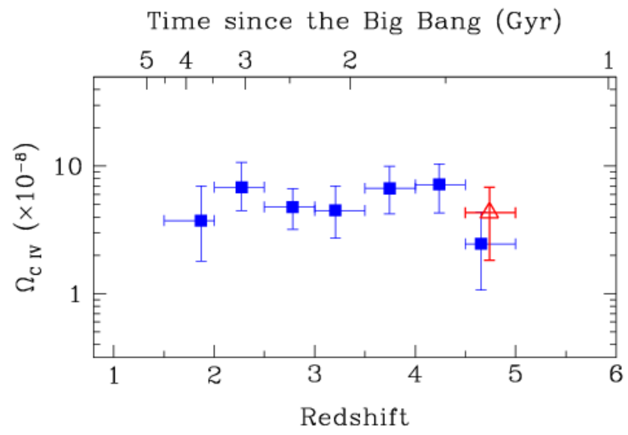

Figure 18: Evolution of mass density of metals from Pettini et al (2003).